

RESEARCH ARTICLE

## Preparation of basil seed mucilage aerogels loaded with paclitaxel nanoparticles by the combination of phase inversion technique and gas antisolvent process

Seyyed Mohammad Ghoreishi\*, Iman Akbari; Ali Hedayati

Department of Chemical Engineering, Isfahan University of Technology, Isfahan, Iran

### ARTICLE INFO

#### Article History:

Received 02 August 2017

Accepted 21 September 2017

Published 27 September 2017

#### Keywords:

Aerogels

Basil seed mucilage (BSM)

Paclitaxel

Gas antisolvent process (GAS)

Supercritical drying

### ABSTRACT

**Objective(s):** In this work, paclitaxel (PX), a promising anticancer drug, was loaded in the basil seed mucilage (BSM) aerogels by implementation of supercritical carbon dioxide (SC-CO<sub>2</sub>) technology. Then, the effects of operating conditions were studied on the PX mean particle size (MPS), particle size distribution (PSD) and drug loading efficiency (DLE).

**Methods:** The employed SC-CO<sub>2</sub> process in this research is the combination of phase inversion technique and gas antisolvent (GAS) process. The effect of DMSO/water ratio (4 and 6 (v/v)), pressure (10-20 MPa), CO<sub>2</sub> addition rate (1-3 mL/min) and ethanol concentration (5-10%) were studied on MPS, PSD and DLE. Scanning electron microscopy (SEM) and Zetasizer were used for particle analysis. DLE was investigated by utilizing the high-performance liquid chromatography (HPLC).

**Results:** TNanoparticles of paclitaxel (MPS of 82-131 nm depending on process variables) with narrow PSD were successfully loaded in BSM aerogel with DLE of 28-52%. Experimental results indicated that higher DMSO/water ratio, ethanol concentration, pressure and CO<sub>2</sub> addition rate reduced MPS and DLE.

**Conclusions:** A modified semi batch SC-CO<sub>2</sub> process based on the combination of gas antisolvent process and phase inversion methods using DMSO as co-solvent and ethanol as a secondary solvent was developed for the loading of an anticancer drug, PX, in ocimum basilicum mucilage aerogel. The experimental results determined that the mean particle size, particle size distribution, and drug loading efficiency be controlled with operating conditions.

#### How to cite this article:

Ghoreishi S M, Akbari I, Hedayati A, Preparation of basil seed mucilage aerogels loaded with paclitaxel nanoparticles by the combination of phase inversion technique and gas antisolvent process. *Nanomed Res J*, 2017; 2(3):179-188. DOI: 10.22034/nmrj.2017.03.006

### INTRODUCTION

Paclitaxel (PX), a promising anticancer drug, is a natural alkaloid belonging to a class of taxanes with excellent therapeutic efficacy against a wide variety of cancers through the inhibition of DNA synthesis by stabilizing microtubule assembly (by interfering with their normal depolymerization) [1-3]. The poor water solubility of PX in conventional vehicles is greatly restricted the significant activity of PX in clinical applications and causes low therapeutic index [4]. Therefore, the use of an adjuvant (Cremophor® EL (polyethoxylated castor oil)) is required in its current formulation which causes

\* Corresponding Author Email: [ghoreishi@cc.iut.ac.ir](mailto:ghoreishi@cc.iut.ac.ir)

several undesirable side effects (including severe hypersensitivity reactions, myelosuppression, and neurotoxicity) [5,6]. Hence, maximizing PX activity and minimizing these side effects by the development of new PX formulations is an important approach.

In recent years, the design of novel drug delivery systems by employing both synthetic (such as PE, PP, and PDMS) and natural polymers have been successfully investigated [7-9]. However, the use of natural origin polymers (plant derived polymers) for pharmaceutical applications are more attractive



This work is licensed under the Creative Commons Attribution 4.0 International License.

To view a copy of this license, visit <http://creativecommons.org/licenses/by/4.0/>.

and regarded as key formulation ingredients for the engineering of modified drug delivery systems. Natural polymers are non-toxic, biocompatible, stable, inexpensive, freely available, potentially biodegradable, and renewable and have the capability of chemical modifications in comparison to synthetic polymers [10-13].

Mucilages are plant derived natural polymers that largely consist of polysaccharides and proteins. Mucilage is a gelatinous substance with wide usages such as adjuvant, thickeners, suspending agents, binders, a granulating agent in the pharmaceutical industries and also used as matrices for sustained and controlled drugs delivery [14- 16].

*Ocimum basilicum* L. (OB) seeds are rich sources of mucilage. OB is an important culinary, aromatic herb which is a native species in tropical and subtropical regions of Asia, Africa, and Central and South America that has several functional characteristics such as treatment of flatulence, gastritis, headaches, coughs, diarrhea, constipation, dyspepsia, warts, worms and kidney malfunctions. It contains a high proportion of phenolic derivatives, aroma compounds and essential oils containing biologically active constituents [17, 18]. The basil seed mucilage can be extracted by soaking the basil seeds in water that results in swelling of outer pericarp into a gelatinous mass which could be concentrated or dried for further applications [19].

Sending the drug to a specific site, in a specific time and release pattern is the goal of an ideal drug delivery system [20-22]. Ion exchange resins [23], films [24], microspheres and gels [25, 26] are some common drug delivery systems that may have many adverse effects (including gastrointestinal or renal side effects). These disadvantages lead to the significant interest in the development of drug delivery systems providing better release rate, reduce toxicity and optimize the drug therapeutics [7].

Application of aerogels as a drug delivery system enhances pharmacokinetic properties, release rate and the bioavailability rate of active pharmaceutical ingredients (API) [27]. There is growing interest in aerogels made of organic materials such as polysaccharides due to their outstanding properties such as low densities, large open pores, high inner surface areas and drug loading capacities, their ability of controlled drug release, capability to

increase the bioavailability of low solubility drugs and improving both their stability and their release kinetics by combining the natural properties of polysaccharides and aerogels structure [28-30].

Aerogels are generally synthesized by direct polymerization of organic precursors followed by solvent exchange and supercritical drying steps or using a conventional sol-gel technique involving subsequent hydrolysis, condensation, gelation, aging and supercritical drying steps [31-33].

Incorporation of drugs into aerogels is applicable by several methods such as the addition of the drug during the synthesis, sol-gel process or during the post-treatment of the synthesized gels or aerogels (supercritical adsorption) [34, 35]. Most of the previous techniques proposed for incorporation of drug samples into the aerogels present some limitations (time-consuming, presence of organic solvents that can remain entrapped inside the polymeric network). Supercritical fluid techniques overcome these disadvantages due to their high dissolving power (liquid-like) and transport properties (gas-like) [36,37]. Supercritical carbon dioxide (SC-CO<sub>2</sub>) is usually preferred in pharmaceutical applications, because of features like non-reactive, non-toxic, non-flammable, environmentally benign, inexpensive, naturally abundance and favorable critical properties [38-41].

Drug loading during the post-treatment is practicable by adsorption of the pharmaceutical compound into the pores of the aerogels via supercritical impregnation. However, limited solubility of most drugs restricted the use of this technique for a wide variety of pharmaceutical compounds. The common supercritical methods is not directly applicable to water soluble polymers (SC-CO<sub>2</sub> shows a very limited compatibility with polar components).

Thus, this work presents the combination of modified semi batch SC-CO<sub>2</sub> assisted phase inversion and gas antisolvent (GAS) process technique for generation and loading of PX nanoparticles into the aerogels of *ocimum basilicum* seeds musilage (BSM), a plant derived low-cost polymer. Our attention was focused on the effect of process variables on the PX particle size and the drug loading efficiency. Moreover, there is no reported study dealing with the PX-loading in BSM-aerogel under Supercritical condition. In the presented work, BSM aerogels

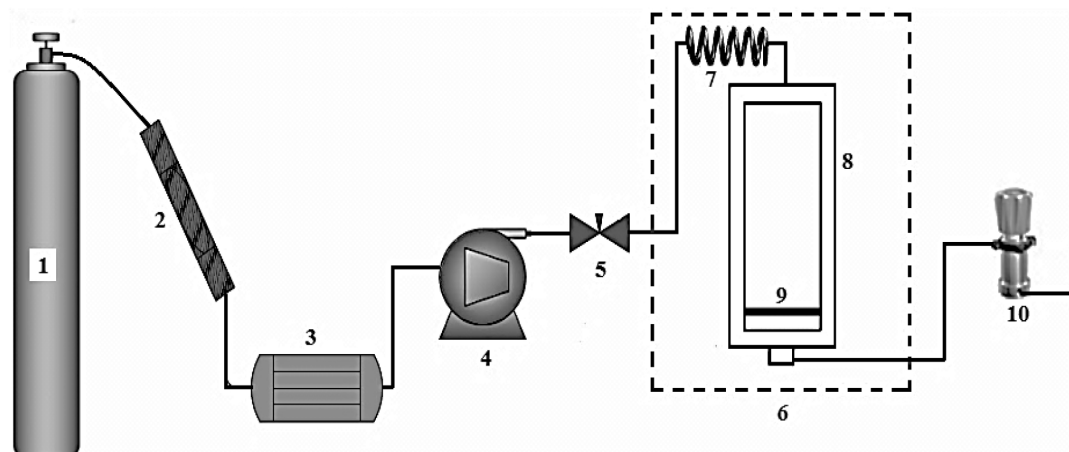


Fig. 1. Schematic diagram of employed SC-CO<sub>2</sub> process; (1) CO<sub>2</sub> cylinder, (2) column consisting of molecular sieve and silica gel, (3) chiller, (4) HPLC pump, (5) needle valve, (6) oven, (7) spring coil preheater, (8) stainless steel high pressure vessel, (9) metallic porous filter, (10) BPR valve.

were used as carriers for PX loading using a newly developed technique. The used SC-CO<sub>2</sub> process in this study is the combination of gas antisolvent (GAS) and phase inversion techniques in two steps: (1) the preparation of casting solution (a uniform mixture of BSM, water, paclitaxel, ethanol and dimethyl sulfoxide (DMSO)), (2) simultaneous generation and precipitation of PX nanoparticles in BSM aerogels using SC-CO<sub>2</sub> (antisolvent). The aim was to design, study, and optimize the process of PX loading on BSM aerogels as an active substance under various operating conditions.

## MATERIALS AND METHODS

Paclitaxel was purchased from Sobhan Oncology Co. (Iran). Basil seeds were prepared from agriculture research center (Isfahan-Iran). Dichloromethane (DCM) ( $\geq 99.9\%$ , Merck, CAS #: 75-09-2), acetonitrile (ACN) ( $\geq 99.9\%$ , Merck, CAS #: 75-05-8), Sodium hydroxide ( $\geq 99.0\%$ , CAS #: 1310-73-2), dimethyl sulfoxide (DMSO) ( $\geq 99.9\%$ , Merck, CAS #: 67-68-5), ethanol ( $\geq 99.9\%$ , CAS #: 64-17-5) and deionized water were used in HPLC analysis and drug loading in aerogels structure. Industrial grade carbon dioxide ( $\geq 99.9\%$ ) was purchased from Ardestan Co. (Isfahan, Iran).

### Supercritical fluid apparatus

The supercritical system in Fig. 1 was used to carry out the objectives of this study. The detailed explanation of apparatus is available in our previous publication [42, 43]. Briefly, The CO<sub>2</sub> in the cylinder (1) was passed through the column

of molecular sieve and metal porous filter (2) for further purification. Then, CO<sub>2</sub> was cooled down (-10 to -5 °C) in a chiller (3) and the liquefied CO<sub>2</sub> was charged to the oven (298–523 ± 0.5 K) (6) through the needle valve (5) by a feed pump (4). CO<sub>2</sub> was heated using spring coil preheater (7) inside the oven before entering the 15 mL stainless steel high-pressure vessel (8). For the collection of PX-loaded BSM-aerogels, a metallic porous disc (9) was placed at the bottom of the vessel. The pressure of the vessel in the process was controlled via back pressure regulator (BPR) valve (10).

### Experimental procedure

The detailed procedure of BSM preparation methods and materials was explained in our previous publication [43]. The combination of gas antisolvent and phase inversion techniques was employed in this research. Casting solution which is a uniform mixture of BSM, water, paclitaxel, dimethyl sulfoxide (DMSO) and ethanol was prepared in the first step, and then simultaneous generation and loading of PX nanoparticles in BSM aerogels were achieved using SC-CO<sub>2</sub> technology. In this work, a mixture of polymer solution (BSM and water), drug and co-solvent (PX and DMSO) and ethanol (secondary solvent) was prepared and processed by SC-CO<sub>2</sub> with the procedure of our previous work on GAS process [40, 42 and 43]. The casting solution for each experiment was prepared as follows: The hydrogel was obtained by dissolving 10 mg of dried BSM powder in 1 mL of deionized water to form a polymeric solution.

The organic co-solvent, DMSO and the secondary solvent (ethanol) were added to the obtained gel under ultra-sonic bath to obtain a uniform solution. For the two sets of experiments, 3 and 5 mL DMSO was added to the obtained solutions, and then for drug loading, 1 mL of a 0.5 mg/mL PX solution in DMSO was added to each sample. The final casting solutions with DMSO to water ratio of 4 and 6 (v/v) and drug to polymer of 5% (w/w) for all samples were prepared. Also, samples with different ethanol concentrations (5, 7.5 and 10% (v/v)) were obtained to investigate its impact on the produced aerogels. The casting solution was loaded into the high-pressure vessel. All experiments were done at a constant temperature of 50 °C which was set by the oven. The vessel was closed via the valve closure, and CO<sub>2</sub> was charged into the vessel. CO<sub>2</sub> injection was continued to reach the appropriate pressure (10, 15 and 20 MPa). After reaching the equilibrium (by turning off the pump for 30 min), the CO<sub>2</sub> addition was carried out at the flow rates of 1, 2 and 3 mL/min. To ensure that a solvent (DMSO/water/ethanol) free product (PX-loaded BSM) has been obtained; flushing with a constant CO<sub>2</sub> flow rate was maintained. To bring back the system to the atmospheric pressure, the vessel depressurization lasted for about 20 min. The samples of the final product (PX-loaded BSM aerogels) were collected for characterization analyses.

#### Characterizations

Scanning Electron Microscope (SEM) was implemented for qualitative observations of the PX nanoparticles shape and aerogels morphology. The obtained products were sputter coated with gold (SC 7620, Quorum Technologies, UK) at 30 mA for 180 s and analyzed by the SEM (DSM 960A, Carl Zeiss AG, Germany). Particle size, particle size distributions, aerogel fiber diameter and fiber diameter distribution, were measured by Zetasizer Nano ZS (Malvern Instruments, Southborough, MA). The PX sample preparation for Zetasizer analyses was carried out via dissolving the PX-loaded BSM aerogels in water to make a dilute gel containing PX particles. PX particles were removed from gel structure into the clear water sample by filtration and washing the diluted gel, and the obtained samples were analyzed by Zetasizer.

#### Drug loading efficiency

Drug loading was determined based on our previous study [43]. The PX loading efficiency in BSM aerogels was determined by high-performance liquid chromatography (HPLC, Jasco, equipped with UV-visible detector). Acetonitrile: water (50:50, v/v) solution was used as the mobile phase. The PX nanoparticles embedded in the BSM aerogel were extracted by dissolution of 2 mg of sample in 1 mL DCM in an ultrasonic low-temperature bath. After allowing the DCM evaporation from the sample, 5 mL of mobile phase was added and placed in an ultrasonic water bath to dissolve the PX. Then, 2 mL of the solution was filtered into HPLC vials by 0.22 μm syringe filters. Determination of PX loading efficiency of each sample was carried out three times for each one. Drug loading efficiency (DLE) was calculated as shown below:

$$DLE (\%) = \frac{\text{Actual loading of PX (mg)}}{\text{Theoretical loading of PX in the casting solution (mg)}} \times 100 \quad (1)$$

## RESULTS AND DISCUSSION

In this study, our attention was focused on the effect of process variables on PX particle size, size distribution, and drug loading efficiency. When the effect of each variable was studied, the values of other variables had been fixed based on one factor at a time method. Triplicate experiments were carried out in each operating condition, and the mean values have been reported throughout the manuscript.

#### Effect of pressure

The effect of pressure at three levels (10, 15 and 20 MPa) was studied at a constant CO<sub>2</sub> flow rate of 2 mL/min, ethanol concentration of 7.5% (v/v), DMSO/water ratio of 6 (v/v) and the temperature of 50 °C. For the lowest (10 MPa) and highest (20 MPa) pressures, mean particle diameters were 130

**Table 1.** Mean particle size of paclitaxel particles and drug loading efficiency obtained at 50 °C, 2 mL/min, DMSO/water ratio of 6 (v/v), ethanol concentration of 7.5% (v/v) and various pressures of 10, 15 and 20 MPa.

Pressure	Mean particle size (nm)	Drug loading efficiency (%)
10	130	49
15	112	45
20	104	43

nm and 104 nm, respectively. Table 1 shows the obtained results of mean particle size and drug loading efficiency for three operating pressures. As illustrated in Table 1, increasing the pressure led to the decreasing of mean particle size. An increase in the pressure increases the supercritical CO<sub>2</sub> density and solvation power. Furthermore, faster supercritical CO<sub>2</sub> extraction of the liquid solvent leads to the rapid supersaturation (enhanced nucleation); thus, the average particle size tends to decrease which was confirmed by the results of this study. As pressure increased from 10 to 20 MPa, the drug loading efficiency decreased from 49% to 43%. Increasing the pressure (increasing SC-CO<sub>2</sub> density) raises PX solubility in SC-CO<sub>2</sub> that leads to PX discharging from the aerogel structure and high-pressure vessel. The remaining experiments were conducted at the constant pressure of 20 MPa.

#### Effect of CO<sub>2</sub> flow rate

The effect of CO<sub>2</sub> addition rate (1, 2 and 3 mL/min) on particle size and drug loading efficiency was investigated at fixed temperature, pressure, DMSO/water ratio and ethanol concentration of 50 °C, 20 MPa, 6 (v/v) and 7.5% (v/v), respectively. For the highest addition rate (3 mL/min), the minimum mean particle size was obtained to be 87 nm. As illustrated in Table 2, increasing the CO<sub>2</sub> addition rate resulted in smaller mean particle size which is similar to conventional GAS processes [40, 42]. At higher CO<sub>2</sub> (antisolvent) addition rate, more volumetric expansion and supersaturation occurred. The rate of supersaturation controlled the nucleation rate and the larger number of nucleus formed with primary nucleation. At this time solute concentration in the liquid phase and the supersaturation were reduced. Due to the production of enough particles with a large surface area, the secondary nucleation could occur. Particle size grows up when there is a concentration driving

**Table 2.** Mean particle size of paclitaxel particles and drug loading efficiency obtained at 50 °C, 20 MPa, DMSO/water ratio of 6 and (v/v), ethanol concentration of 7.5% (v/v) and CO<sub>2</sub> flow rates of 1, 2 and 3 mL/min.

CO <sub>2</sub> flow rate (mL/min)	Mean particle size (nm)	Drug loading efficiency (%)
1	131	52
2	104	43
3	87	38

force in the solution and particle surface. However, in this case, the high CO<sub>2</sub> addition rate discharged the supersaturation, so, the nucleation mechanism prevailed and growth rate decreased.

As indicated in Table 2, drug loading efficiency decreased when the CO<sub>2</sub> addition rate increased. Higher CO<sub>2</sub> flow rate (the low average residence time) and the subsequent turbulency discharges the smaller PX particles from the vessel, and consequently, the PX particles are not precipitated in the BSM aerogel which leads to the decreased drug loading efficiency. The CO<sub>2</sub> addition rate of 3 ml/min was used for the rest of experiments.

#### Effect of co-solvent (DMSO) to water ratio and ethanol concentration

In this research, DMSO was simultaneously used as a solvent for PX based on the GAS technique and also as co-solvent due to its appropriate PX solubility and relative compatibility with water for increasing water solubility in SC-CO<sub>2</sub> based on phase inversion method. The amount of co-solvent directly affects the obtained structure, particle size distribution, and drug loading efficiency. By implementation of DMSO/water < 2 (v/v), the water content of polymer solution could not be removed by the non-solvent stream (DMSO/SC-CO<sub>2</sub> mixture) in a reasonable time (less than 2 h). Also, for the DMSO/water > 7 (v/v), a two phase mixture of casting solution was prepared (casting solution was not uniform), a phase poor in BSM and

**Table 3.** Mean particle size and drug loading efficiency of paclitaxel particles and specific volume (cm<sup>3</sup>/g) of BSM aerogels obtained at 50 °C, 3 mL/min, 20 MPa, DMSO/water ratios of 4 and 6 (v/v) and ethanol concentrations of 5, 7.5 and 10%.

Ethanol concentration (%)	DMSO/water=6 (v/v)			DMSO/water=4 (v/v)		
	Mean particle diameter (nm)	Drug loading efficiency	Specific volume (cm <sup>3</sup> /g)	Mean particle diameter (nm)	Drug loading efficiency	Specific volume (cm <sup>3</sup> /g)
5	113	49	186.9	128	45	109.6
7.5	87	38	300.0	88	42	280.3
10	82	28	319.3	84	34	306.4

another phase rich in BSM [43]. Thus, experiments were carried out in two levels of DMSO/water ratio of 4 and 6 (v/v) while the ethanol concentration was in the range of 5-10% (v/v).

Table 3 shows the obtained results for mean particle size and drug loading efficiency of paclitaxel particles and specific volume (cm<sup>3</sup>/g) of BSM aerogels obtained at 50 °C, 3 mL/min, 20 MPa, DMSO/water ratios of 4 and 6 (v/v) and ethanol concentrations of 5, 7.5 and 10%. As DMSO/water ratio increased from 4 to 6 (v/v), the mean particle size decreased (from 128 to 113 nm (Ceth=5%), from 88 to 87 nm (Ceth=7.5%) and from 84 to 82 (Ceth=10%)). At higher DMSO/water ratio, the PX (solute) concentration decreased in the solution while the amounts of PX and ethanol were kept constant. When the solute (PX) concentration reduces, the nucleation is obtained at the higher volume expansion that leads to the lower rate of nucleus growth. Thus, at higher DMSO/water ratio (lower solute concentration), the smaller particles generation is expected which is confirmed by the results of this study.

Increasing the ethanol concentration in both DMSO/water ratios, resulted in increasing the specific volume (decreasing the density) of the produced aerogels. The diffusion of the supercritical mixture (SC-CO<sub>2</sub>/ethanol) in the hydrogel structure generated more porous and low density (high specific volume) BSM aerogels. There was more deviation between the aerogels specific volumes of the two DMSO/water ratios of 4 and 6 (v/v) in ethanol concentration of 5% in comparison to the higher ethanol concentrations. This showed that in lower ethanol concentrations, DMSO acts as an auxiliary agent for expansion. By increasing the ethanol concentration in the vessel, the influence of DMSO on the production of porous structure vanishes.

Fig. 2 shows the SEM image of the obtained product from DMSO/water ratio of 6 (v/v), ethanol concentration of 7.5%, pressure of 20 MPa, the

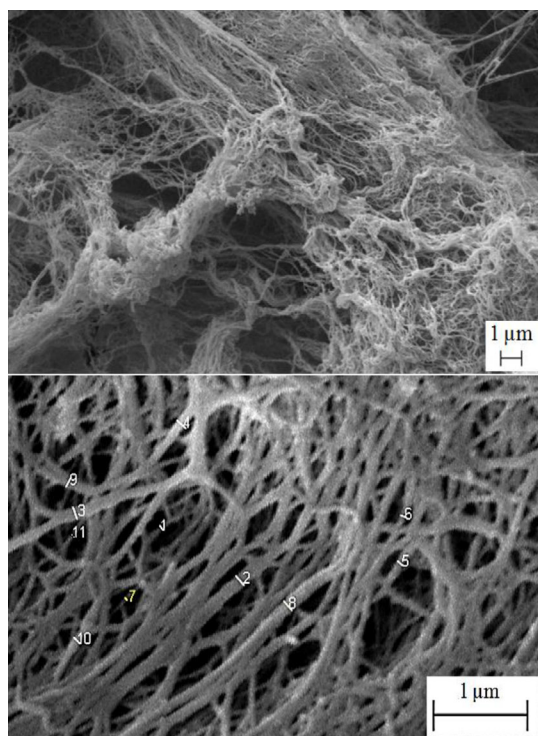


Fig. 2. SEM image of paclitaxel loaded BSM aerogel obtained at 50 °C, CO<sub>2</sub> flow rate of 3 mL/min, 20 MPa, ethanol concentration of 7.5% and DMSO/water ratio of 6 (v/v) with the magnitude of a) 10000X and b) 25000X.

temperature of 50 °C and CO<sub>2</sub> flow rate of 3 ml/min. Image J software was used for the aerogel fibers diameter determination.

The diameters of determined fibers in Fig. 2.b have been shown in Table 4. As illustrated in Table 4, the diameter of aerogel fibers varied from 30 nm to 121 nm. The mean fiber diameter of aerogels was also determined by means of 160 randomly chosen points.

Fig. 3 shows the fiber diameter distribution in the BSM aerogels at 50°C, 3 mL/min, 20 MPa, 7.5% ethanol and DMSO/water of 6 (v/v).

Fig. 4 and 5 show particle size distribution for three levels of ethanol concentration (5, 7.5 and 10%) in DMSO to water ratio of 4 and 6 (v/v), respectively.

**Table 4.** The diameter of the fibers shown in Fig. 2.b at 50 °C, CO<sub>2</sub> flow rate of 3 mL/min, 20 MPa, ethanol concentration of 7.5% and DMSO/water ratio of 6 (v/v)

number	1	2	3	4	5	6	7	8	9	10	11
Fiber diameter (nm)	45	120	114	121	68	64	30	120	100	87	37

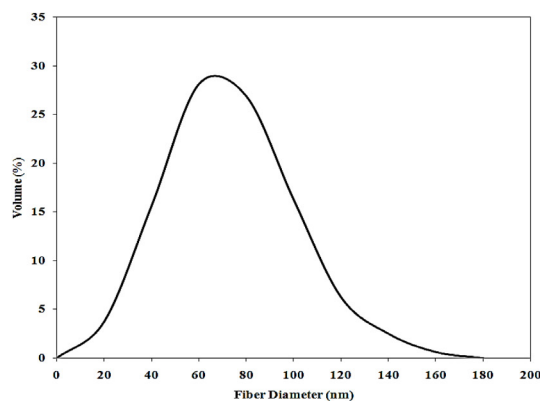


Fig. 3. diameter distribution of aerogel fibers obtained at 50 °C, 3 mL/min, 20 MPa, 7.5% ethanol and DMSO/water of 6 (v/v).

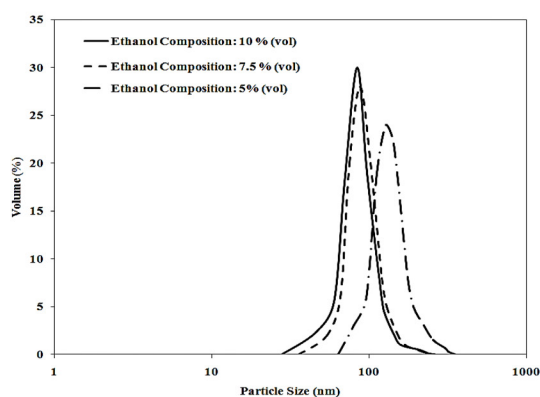


Fig. 4. Size distribution of paclitaxel particles obtained at 50 °C, 3 mL/min, DMSO/water ratio of 4 (v/v) and various ethanol concentrations of 5, 7.5 and 10%.

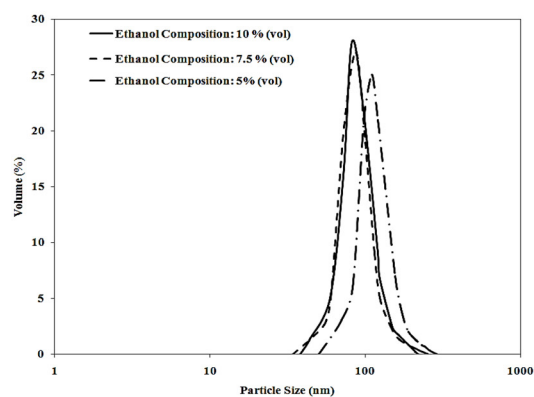


Fig. 5. Size distribution of paclitaxel particles obtained at 50 °C, 3 mL/min, DMSO/water ratio of 6 (v/v) and various ethanol concentrations of 5, 7.5 and 10%.

Increasing the ethanol concentration lowered the PX mean particle diameters from 113 to 82 nm (DMSO/water=6%) and from 128 to 84 nm (DMSO/water=4%) while drug loading efficiency decreased from 49 to 28% (DMSO/water=6%) and from 45 to 34% (DMSO/water=4%). Therefore, a counter effect was observed regarding the effect of ethanol concentration on drug loading efficiency and particle size. It is necessary to realize that the lower PX concentration decreases the particle size which results in an increased surface area and dissolution rate.

At higher ethanol concentrations, much more unsaturated PX particles were carried out by ethanol in the outlet stream, and thus the precipitation of PX in the BSM aerogel was inhibited. This phenomenon explains the lower PX loading efficiency at higher ethanol concentrations which is confirmed by the results of this study. When initial solute (PX) concentration increased

by decreasing the ethanol concentration, the nucleation obtained at the lower volume expansion. Therefore, the nucleuses grow in a longer time, and larger PX nanoparticles will be produced. By increasing the ethanol concentration from 5 to 7.5%, the solute concentration decreased (more volume expansion) and resulted in enhanced particle growth rate. However, by increasing the ethanol concentration from 7.5 to 10%, no significant change in the particle size was observed. The SEM image of the loaded and encapsulated PX particles in the aerogel structure in DMSO/water ratio of 6 (v/v), ethanol concentration of 7.5% (v/v), pressure of 20 MPa, temperature of 50 °C and CO<sub>2</sub> flow rate of 3 ml/min was shown in Fig. 6.

Our experiments showed that the addition of a secondary solvent (ethanol in this case) to the casting solution causes the expansion in the BSM polymer structure and results in the production of BSM aerogel while without using ethanol in the casting

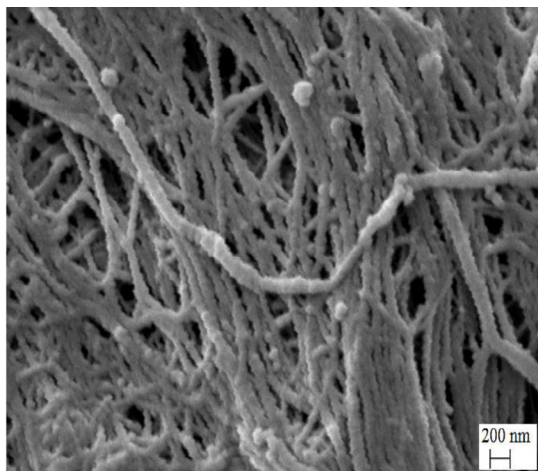


**Fig. 6.** SEM image of the loaded PX particles in the aerogel structure in DMSO/water ratio of 6 (v/v), ethanol concentration of 7.5%, the pressure of 20 MPa, the temperature of 50 °C and CO<sub>2</sub> flow rate of 3 mL/min.

solution there will be a non-porous polymeric structure [43] with very different properties. To overcome the shrinkage of precipitated filaments, and to obtain a nanoporous structure with high porosity (BSM aerogel) the drying procedure was carried out using SC-CO<sub>2</sub> by the addition of organic solvent to the casting solution. The addition of an organic solvent readily soluble in SC-CO<sub>2</sub> to the water eliminated the solubility problem of water in CO<sub>2</sub>. In this case, the 3-D shape and the sample size not only was successfully preserved, but also increased in size due to diffusion of SC-CO<sub>2</sub> in gel structure. The volume expansion of solution, water and ethanol in this case, leads to expansion of polymer structure and thus high level of porosity was obtained using SC-CO<sub>2</sub> gel drying method and also lower paclitaxel nanoparticle mean particle size was obtained in contrast to our previous work for the precipitation of drug sample into the non-porous polymeric structure of basil seed mucilage [43]. Furthermore, during the expansion, because of high diffusivity, supercritical mixture diffuse to the polymer structure and thus nanometric fibers and pores were obtained.

To ensure complete removal of PX nanoparticles from the BSM aerogel for drug loading calculations, the PX-free BSM (from the first step) was dried, and the residual amount of PX nanoparticles were obtained in the similar procedure for drug loading measurement. The total PX residual in the BSM matrix must not be more than 2 percent of the

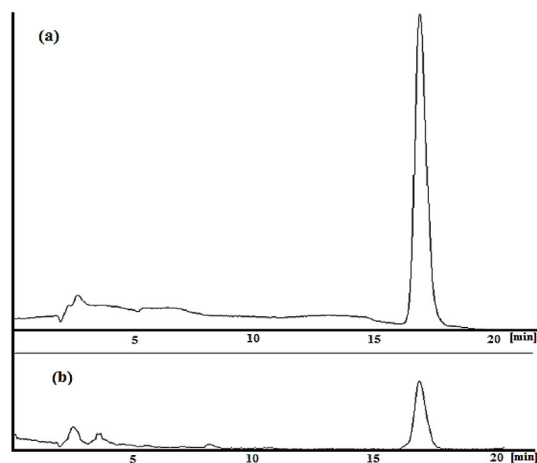


**Fig. 7.** The chromatogram of a) unprocessed and b) processed paclitaxel in DMSO/water ratio of 6 (v/v), ethanol concentration of 7.5%, pressure of 20 MPa, the temperature of 50 °C and CO<sub>2</sub> flow rate of 3 mL/min.

theoretical amount of loaded PX.

Fig. 7 illustrates the chromatogram of unprocessed (as the reference sample) and processed paclitaxel using the supercritical technique for PX loading into BSM aerogels. Mobile phase, mobile phase velocity, temperature, detector and injected volume were: acetonitrile: water (50:50, v/v), 1 mL/min, ambient temperature, UV detector with 227 nm wavelength and 20 μL, respectively. Based on Fig. 7, both chromatograms have the same retention time of 17 min and show no changes in drug (PX) structure after all processes.

## CONCLUSIONS

A modified semi batch SC-CO<sub>2</sub> process based on the combination of gas antisolvent process and phase inversion methods using DMSO as co-solvent and ethanol as a secondary solvent was developed for the loading of an anticancer drug, PX, in *ocimum basilicum* mucilage aerogel. According to the process variables, PX nanoparticles with mean particle size of 82-131 nm and narrow particle size distribution with DLE of 28–52% were successfully loaded in BSM aerogels. The experimental results determined that the mean particle size, particle size distribution, and drug loading efficiency be controlled with operating conditions. PX mean particle size was decreased at higher DMSO/water ratio. In the same manner, lower pressure, ethanol concentration and CO<sub>2</sub> addition rate increased the particle size and the drug loading efficiency.

## ACKNOWLEDGEMENTS

The financial support provided by Isfahan University of Technology is gratefully acknowledged.

## CONFLICT OF INTEREST

The authors declare that there are no conflicts of interest regarding the publication of this manuscript.

## REFERENCES

1. Ravar F, Saadat E, Gholami M, Dehghankelishadi P, Mahdavi M, Azami S, Dorkoosh FA. Hyaluronic acid-coated liposomes for targeted delivery of paclitaxel, in-vitro characterization and in-vivo evaluation. *Journal of Controlled Release*, 2016;229:10-22.
2. Li S, Wang X, Li W, Yuan G, Pan Y, Chen H. Preparation and characterization of a novel conformed bipolymer paclitaxel-nanoparticle using tea polysaccharides and zein, *Carbohydrate polymers*, 2016;146:52-7.
3. Nasiri J, Motamedi E, Naghavi MR. Comparative study of adsorptive role of carbonaceous materials in removal of UV-active impurities of paclitaxel extracts, *Journal of Pharmaceutical Analysis*, 2015;5(6):396-9.
4. Szczepanowicz K, Bzowska M, Kruk T, Karabasz A, Bereta J, Warszynski P. Pegylated polyelectrolyte nanoparticles containing paclitaxel as a promising candidate for drug carriers for passive targeting, *Colloids and Surfaces B: Biointerfaces*, 2016;143:463-71.
5. Chen N, Guo D, Guo Y, Sun Y, Bi H, Ma X. Paclitaxel inhibits cell proliferation and collagen lattice contraction via TGF- $\beta$  signaling pathway in human tenon's fibroblasts in vitro, *European journal of pharmacology*, 2016;777:33-40.
6. Esfandyari-Manesh M, Darvishi B, Ishkuh FA, Shahmoradi E, Mohammadi A, Javanbakht M, Dinarvand R, Atyabi F. Paclitaxel molecularly imprinted polymer-PEG-folate nanoparticles for targeting anticancer delivery: characterization and cellular cytotoxicity, *Materials Science and Engineering: C*, 2016;62:626-33.
7. Zhao J, Lu C, He X, Zhang X, Zhang W, Zhang X. Polyethylenimine-grafted cellulose nanofibril aerogels as versatile vehicles for drug delivery, *ACS applied materials & interfaces*, 2015;7(4):2607-15.
8. Sanyakamdorn S, Agudelo D, Bekale L, Tajmir-Riahi HA. Targeted conjugation of breast anticancer drug tamoxifen and its metabolites with synthetic polymers, *Colloids and Surfaces B: Biointerfaces*, 2016;145:55-63.
9. Singh B, Sharma V. Designing galacturonic acid/arabinogalactan crosslinked poly (vinyl pyrrolidone)-co-poly (2-acrylamido-2-methylpropane sulfonic acid) polymers: Synthesis, characterization and drug delivery application, *Polymer*, 2016;91:50-61.
10. Pillai O, Panchagnula R. Polymers in drug delivery, *Journal of Materials Science: Materials in Medicine*, 2001;5(4):447-51.
11. Sadri M, Mohammadi A, Hosseini H. Drug release rate and kinetic investigation of composite polymeric nanofibers, *Nanomedicine Research Journal*, 2016;1(2):112-21.
12. García-González CA, Alnaief M, Smirnova I. Polysaccharide-based aerogels-Promising biodegradable carriers for drug delivery systems, *Carbohydrate Polymers*, 2011;86(4):1425-38.
13. Volokitina MV, Korzhikov-Vlakh VA, Tennikova TB, Korzhikova-Vlakh EG. Macroporous monoliths for biodegradation study of polymer particles considered as drug delivery systems, *Journal of pharmaceutical and biomedical analysis*, 2017;145:169-77.
14. Prajapati VD, Jani GK, Moradiya NG, Randeria NP. Pharmaceutical applications of various natural gums, mucilages and their modified forms, *Carbohydrate polymers*, 2013;92(2):1685-99.
15. Kaewmanee T, Bagnasco L, Benjakul S, Lanteri S, Morelli CF, Speranza G, Cosulich ME. Characterisation of mucilages extracted from seven Italian cultivars of flax. , *Food Chem.* 2014 Apr 1;148:60-9.
16. Nayak AK, Pal D, Das S. Calcium pectinate-fenugreek seed mucilage mucoadhesive beads for controlled delivery of metformin HCl, *Food chemistry*, 2013;96(1):349-57.
17. Bhuvaneshwari K, Gokulanathan A, Jayanthi M, Govindasamy V, Milella L, Lee S, Yang DC, Girija S. Can *Ocimum basilicum* L. and *Ocimum tenuiflorum* L. in vitro culture be a potential source of secondary metabolites?, *Food chemistry*, 2016;194:55-60.
18. Kadan S, Saad B, Sasson Y, Zaid H. In vitro evaluation of anti-diabetic activity and cytotoxicity of chemically analysed *Ocimum basilicum* extracts, *Food Chemistry*, 2016;196:1066-74.
19. Jouki M, Mortazavi SA, Yazdi FT, Koocheki A. Optimization of extraction, antioxidant activity and functional properties of quince seed mucilage by RSM, *International Journal of Biological Macromolecules*, 2014;66:113-24.
20. Mahdavinia GR, Afzali A, Etemadi H, Hoseinzadeh H. Magnetic/pH-sensitive nanocomposite hydrogel based carboxymethyl cellulose-g-polyacrylamide/montmorillonite for colon targeted drug delivery. *Nanomedicine Research Journal*, 2017;2(2):111-22.
21. Amoli Diva M, Pourghazi K. Magnetic nanoparticles grafted pH-responsive poly (methacrylic acid-co-acrylic acid)-grafted polyvinylpyrrolidone as a nano-carrier for oral controlled delivery of atorvastatin, *Nanomedicine Research Journal*, 2017;2(1):18-27.
22. Najafi-Taher R, Amani A. Nanoemulsions: colloidal topical delivery systems for antiacne agents-A Mini-Review,

- Nanomedicine Research Journal, 2017;2(1):49-56.
23. Anand V, Kandarapu R, Garg S. Ion-exchange resins: carrying drug delivery forward, *Drug Discovery Today*, 2001;6(17):905-14.
  24. Kolakovic R, Peltonen L, Laukkanen A, Hirvonen J, Laaksonen T. Nanofibrillar cellulose films for controlled drug delivery, *European Journal of Pharmaceutics and Biopharmaceutics*, 2012;82(2):308-15.
  25. Amin MC, Ahmad N, Halib N, Ahmad I. Synthesis and characterization of thermo- and pH-responsive bacterial cellulose/acrylic acid hydrogels for drug delivery, *Carbohydrate Polymers*, 2012;88(2):465-73.
  26. Valo H, Arola S, Laaksonen P, Torkkeli M, Peltonen L, Linder MB, Serimaa R, Kuga S, Hirvonen J, Laaksonen T, *European Journal of Pharmaceutical Sciences*, 2013;50: 69-77.
  27. Lovskaya DD, Lebedev AE, Menshutina NV. Aerogels as drug delivery systems: in vitro and in vivo evaluations, *The Journal of Supercritical Fluids*, 2015;106:115-21.
  28. Ulker Z, Erkey C. Experimental and theoretical investigation of drug loading to silica aerogels, *The Journal of Supercritical Fluids*, 2015, 31;106:34-41.
  29. García-González CA, Jin M, Gerth J, Alvarez-Lorenzo C, Smirnova I. Polysaccharide-based aerogel microspheres for oral drug delivery, *Carbohydrate polymers*, 2015;117:797-806.
  30. Pantić M, Knez Ž, Novak Z. Supercritical impregnation as a feasible technique for entrapment of fat-soluble vitamins into alginate aerogels, *Journal of non-crystalline solids*, 2016;432:519-26.
  31. Wang R, Shou D, Lv O, Kong Y, Deng L, Shen J. pH-Controlled drug delivery with hybrid aerogel of chitosan, carboxymethyl cellulose and graphene oxide as the carrier, *International Journal of Biological Macromolecules*, 2017;103:248-53.
  32. Veres P, Kéri M, Bányai I, Lázár I, Fábrián I, Domingo C, Kalmár J. Mechanism of drug release from silica-gelatin aerogel—Relationship between matrix structure and release kinetics, *Colloids and Surfaces B: Biointerfaces*, 2017;152:229-37.
  33. Eleftheriadis GK, Filippousi M, Tsachouridou V, Darda MA, Sygellou L, Kontopoulou I, Bouropoulos N, Steriotis T, Charalambopoulou G, Vizirianakis IS, Van Tendeloo G. Evaluation of mesoporous carbon aerogels as carriers of the non-steroidal anti-inflammatory drug ibuprofen, *International journal of pharmaceutics*, 2016;515(1):262-70.
  34. Marin MA, Mallepally RR, McHugh MA. Silk fibroin aerogels for drug delivery applications, *The Journal of Supercritical Fluids*, 2014;91:84-9.
  35. Del Gaudio P, Auriemma G, Mencherini T, Porta GD, Reverchon E, Aquino RP. Design of alginate-based aerogel for nonsteroidal anti-inflammatory drugs controlled delivery systems using prilling and supercritical-assisted drying, *Journal of pharmaceutical sciences*, 2013;102(1):185-94.
  36. Ghoreishi SM, Hedayati A, Mohammadi S. Optimization of periodic static-dynamic supercritical CO<sub>2</sub> extraction of taxifolin from pinus nigra bark with ethanol as entrainer, *The Journal of Supercritical Fluids*, 2016;113:53-60.
  37. Ghoreishi SM, Hedayati A, Mousavi SO. Quercetin extraction from Rosa damascena Mill via supercritical CO<sub>2</sub>: Neural network and adaptive neuro fuzzy interface system modeling and response surface optimization, *The Journal of Supercritical Fluids*, 2016;112:57-66.
  38. Ghoreishi SM, Hedayati A, Kordnejad M. Micronization of chitosan via rapid expansion of supercritical solution, *The Journal of Supercritical Fluids*, 2016;111:162-70.
  39. Esfandiari N, Ghoreishi SM. Synthesis of 5-fluorouracil nanoparticles via supercritical gas antisolvent process, *The Journal of Supercritical Fluids*, 2013;84:205-10.
  40. Esfandiari N, Ghoreishi SM. Ampicillin Nanoparticles Production via Supercritical CO<sub>2</sub> Gas Antisolvent Process, *AAPS PharmSciTech*, 2015;16(6):1263-9.
  41. Akbari I, Ghoreishi SM, Habibi N. Supercritical CO<sub>2</sub> Generation of Nanometric Structure from Ocimum basilicum Mucilage Prepared for Pharmaceutical Applications. *AAPS PharmSciTech*. 2015 Apr 1;16(2):428-34.
  42. Esfandiari N, Ghoreishi SM. Kinetics modeling of ampicillin nanoparticles synthesis via supercritical gas antisolvent process, *The Journal of Supercritical Fluids*, 2013;81:119-27.
  43. Akbari I, Ghoreishi SM, Habibi N. Generation and precipitation of paclitaxel nanoparticles in basil seed mucilage via combination of supercritical gas antisolvent and phase inversion techniques, *The Journal of Supercritical Fluids*, 2014;94:182-8.